*Journal of Molecular Liquids*, 33 (1987) 255—269
Elsevier Science Publishers B.V., Amsterdam — Printed in The Netherlands



# POWER REFLECTIVITY OF LOW DIMENSIONAL SURFACE MATERIALS

M. W. EVANS

Dept. of Physics, University College of Swansea, Swansea SA2 8PP

(Received 20 August 1986)

ABSTRACT

The power reflection coefficient in pi and sigma polarisation is shown to be a potentially useful method of analysing and investigating the properties of surface low dimensional layers. By using the admittance method to convert the complex dielectric permittivity to power reflectivity for a thin layer of material on aluminium substrate it is shown that the various observable features in the dielectric spectrum are to be found also in reflectivity, especially in pi polarisation near the Brewster angle. This result is potentially useful for the detection of surface layers as little as one angstrom in thickness.

## INTRODUCTION

Recent work on power reflectivity from surfaces on highly reflecting substrates has revealed [1-4] the presence of a new spectral feature which could be of experimental interest across the electromagnetic range. In this work a theoretical method was developed, based on the optical admittance, [5,6] to investigate optical reflectance and transmittance at arbitrary angles of incidence of stratified and in general inhomogeneous media with arbitrary refractive index profiles. This method introduces two new variables, capable of providing a great deal more information per experiment than conventional normal angle reflectivity in the infra red and other frequency ranges. These variables are:

i) angle of incidence;

ii) polarisation of the incoming beam, reflected from surface layers as thin as one angstrom.

A mathematical technique has been developed [4-6] to solve Maxwell's equations for reflection from the surface low dimensional film deposited on a homogeneous or inhomogeneous substrate. An algorithm has been developed to

compute the power reflectivity in pi and sigma polarisation for test conditions in the infra red, far infra red and microwave frequency ranges. The results of this work have shown that:

i) reflectivity structure as a function of incidence angle and polarisation, together with surface layer thickness, can be used to predict the reflectivity spectrum as a new analytical technique, provided the experimental research and development is carried out;

ii) a sharp high frequency feature has been detected [1,2] which is associated with the frequency at which the dielectric permittivity of the surface film changes from negative to positive on the high frequency side of the dielectric loss peak. Such a property can occur whenever there are sharp infra-red peaks, such as those in solid low dimensional surface material at low temperature. This is an original discovery of the theoretical work which is pursued further in this paper for more complex types of infra red and far infra red spectra containing more than one peak. The shape and contrast of the new reflectivity feature is strongly dependent, theoretically, on polarisation, angle of incidence, and thickness of the surface layer. The reflectivity is also dependent on the nature of the substrate, and particularly so near the Brewster angle of the substrate in pi polarisation. One interferometric spectrometer could therefore provide a great deal of information in this way from the analysis of reflectivity from surfaces deposited on, for example, metallic substrates. The theory predicts that the technique is sensitive to films of as little as one angstrom in thickness.

In this paper the dielectric loss and permittivity is synthesised on the computer using for each peak an expression based on a suitable truncation of the relevant Mori continued fraction, [7] i.e. that for the orientational (or dipole) autocorrelation function. This allows the study of the high frequency reflectivity feature as a function of peak separation, peak frequency and half width, of surface film thickness, angle of incidence and substrate dielectric properties. These are all variables which can be experimentally controlled, and are therefore potentially useful in the analysis of low dimensional surface material.

## SUMMARY OF THEORY

The theory used to generate the reflectivity spectra from the given dielectric loss and permittivity is described in detail elsewhere. [4] For convenience, a brief summary is given in this section.

The electric and magnetic field vectors $\underset{\sim}{E}$ and $\underset{\sim}{H}$ of angular frequency $\underset{\sim}{\omega}$ obey the following differential equations in an inhomogeneous medium of relative permittivity $\hat{\epsilon}$ (usually a complex function) and a relative permeability of $\mu(=1)$:

$$\Delta\underset{\sim}{E} + (\omega^2/c^2)\hat{\epsilon}\underset{\sim}{E} - \text{grad div } \underset{\sim}{E} = \underset{\sim}{o} \tag{1}$$

$$\Delta\underset{\sim}{H} + (\omega^2/c^2)\hat{\epsilon}\underset{\sim}{H} + (1/\epsilon)(\text{grad } \hat{\epsilon} \times \text{rot } \underset{\sim}{H}) = \underset{\sim}{o} \tag{2}$$

It is assumed that the system is infinite in directions z and y and inhomogeneous only in axis z:

$$\hat{\epsilon} = \hat{\epsilon}(z) \tag{3}$$

The interfaces in the system are parallel to plane (x,y) and the surface layer is on a homogeneous substrate, in this paper aluminium metal. In the theory the dependence of the field vector on z will be treated separately for $\sigma$ and $\pi$ polarisation. In $\pi$ polarisation the electric field is parallel to the plane of incidence, and for $\sigma$ polarisation perpendicular. The $\sigma$ polarisation corresponds to the transverse electric (TE) mode with $\underset{\sim}{E}$ in direction y and the $\pi$ polarisation to the transverse magnetic (TM) with $\underset{\sim}{H}$ in direction y. The transverse field components $E_y$ and $H_y$ then obey the following differential equations:

$$\frac{\partial^2 E_y}{\partial z^2} + \frac{\omega^2}{c^2}(\hat{\epsilon} - \sin^2\phi_o)E_y = o \tag{4}$$

$$\frac{\partial}{\partial z}\left(\frac{1}{\hat{\epsilon}}\frac{\partial H_y}{\partial z}\right) + \frac{\omega^2}{c^2}\left(1 - \frac{\sin^2\phi_o}{\hat{\epsilon}}\right)H_y = o \tag{5}$$

If the admittance function is defined as

$$\hat{j}(z) = -\left(\frac{\mu_o}{\epsilon_o}\right)^{\frac{1}{2}} \frac{H_t(z)}{E_t(z)} , \tag{6}$$

then according to the boundary conditions of Maxwell's equations $H_t$ and $E_t$ are transverse components which are continuous and therefore $\hat{j}(z)$ is also a continuous function of z in the system, unless $E_t=0$ when the admittance function becomes infinite. The interaction of electromagnetic radiation with the inhomogeneous system can then be described [4] with the following differential equations in the admittance function:

$$dj_{TE}/dz = - (i\omega/c) [\hat{\varepsilon} - \sin^2\phi_o - \hat{j}_{TE}^2] \quad (7)$$

$$d\hat{j}_{TM}/dz = - (i\omega/c) [(1 - \frac{\sin^2\phi_o}{\hat{\varepsilon}}) \hat{j}_{TM}^2 - \hat{\varepsilon}] \quad (8)$$

These equations can then be solved using the methods of Hild and Grofscik [5] and this method is described fully for epitaxial semiconductors in a recent paper by Hild and Evans. [4]

## OPTICAL COEFFICIENTS OF PURE ALUMINIUM IN THE REGION BELOW 200 $cm^{-1}$.

The optical coefficients of pure metallic aluminium have recently been investigated thoroughly [8] from the far infra red to the ultra violet, and it can be estimated that the permittivity up to about 200 $cm^{-1}$ is approximately constant at roughly 1.5 and that the dielectric loss is approximately constant at about 320,000. The aluminium substrate is therefore a highly absorbing and reflecting medium in the far infra red in sigma polarisation at all incidence angles. In pi polarisation in contrast, the reflectivity of aluminium drops to near zero for all frequencies up to 200 $cm^{-1}$ for incidence angles near the Brewster angle of

$$\tan^{-1} 320{,}000^{\frac{1}{2}} = 89.8987^o \quad (9)$$

and rapidly rises to unity as the incidence angle becomes $90^o$, i.e. parallel to the surface. (Note that this property is in itself of practical importance in measuring the dielectric loss and permittivity of a metal in the far infra red and microwave).

## SYNTHESIS OF THE DIELECTRIC LOSS AND PERMITTIVITY OF THE SURFACE LAYER

In this section the overall aim is to give an account of the way in which the two peaked infra red spectrum is synthesised in this paper expressly for the purpose of estimating theoretically the effect of inter peak separation, half width, and relative peak height on the reflectivity in pi and sigma polarisation. The dielectric loss and permittivity in this section therefore refers specifically to the surface film. Two methods of synthesis are used, both based on approximants [7] of the continued fraction expansion in Laplace space of the dipole (orientational) correlation function. For the present purpose it is sufficient to take a linear expansion, so that the Laplace transforms $\bar{C}_u(s)$ of the orientational autocorrelation function is:

$$\underset{\sim}{C}_{u}(s) = \cfrac{\underset{\sim}{C}_{u}(o)}{\cfrac{\phi_o(o)}{s+\phi_1(o)}} \qquad (10)$$

$$\vdots$$

In this continued fraction the $\phi_o(o)$ and $\phi_1(o)$ coefficients are equilibrium averages which are defined fully in the literature [7] in terms of intra and inter molecular quantities such as the moment if inertia distribution and the inter molecular mean square torque. In eqn. 1 the continued fraction can be truncated at an approximant defined by the parameter $\gamma$ which is the correlation frequency of a memory function [9] . This type of continued fraction has been truncated at two levels for each peak, whose position and half width; and relative frequency separation, can be defined therefore by the parameters of the continued fraction.

TRUNCATION AT THE SECOND APPROXIMANT

This produces the result

$$\underset{\sim}{C}^{(1)}_{u}(s) = \frac{(s + \gamma_1)}{s(s+\gamma_1)+\phi_o(o)} \qquad (11)$$

so that the dielectric loss and permittivity of the surface film are, respectively:

$$\varepsilon''(\omega) = \frac{\gamma_1\phi_o(o)\omega}{(\phi_o(o) - \omega^2)^2 + \omega^2\gamma_1^2} \qquad (12)$$

and

$$\varepsilon'(\omega) = \varepsilon_o - \frac{(\varepsilon_o-\varepsilon_\infty)\omega^2(\gamma_1^2-\phi_o(o) + \omega^2)}{(\phi_o(o)-\omega^2)^2 + \omega^2\gamma_1^2} \qquad (13)$$

for each peak. The final synthetic absorption and dispersion spectrum of the surface film is therefore a simple sum of both sets of individual peaks. Finally, using equns (12) and (13) with (7) and (8) produces the power reflectivity in sigma and pi polarisation of a thin film of material of this dielectric loss and permittivity deposited as a thin film on pure aluminium substrate.

TRUNCATION AT THE THIRD APPROXIMANT

This produces the following results [7] for the dielectric loss and permittivity

$$\varepsilon''(\omega) = \frac{\gamma_2\phi_o(o)\phi_1(o)\omega(\varepsilon_o-\varepsilon_\infty)}{\gamma_2^2(\phi_o(o)-\omega^2)^2+\omega^2(\omega^2-(\phi_o(o)+\phi_1(o)))^2} \tag{14}$$

and

$$\varepsilon'(\omega) = \varepsilon_o - \frac{(\varepsilon_o-\varepsilon_\infty)\omega^2(\gamma_2^2(\omega^2-\phi_o(o))+(\omega^2-\phi_1(o))(\omega^2-(\phi_o(o)+\phi_1(o))))}{\gamma_2^2(\phi_o(o)-\omega^2)^2+\omega^2(\omega^2-(\phi_o(o)+\phi_1(o))^2} \tag{15}$$

respectively.

The two peaked far infra red spectrum is in this case synthesised from a combination of the sets of parameters $\phi_o(o)$, $\phi_1(o)$ and $\gamma_2$ which control the overall appearance of the spectrum. The power reflectivity is finally computed from the dielectric loss and permittivity by using equns (14) and (15) for the two peaks in equns (7) and (8).

RESULTS AND DISCUSSION

The results for the dielectric loss and permittivity dispersion in fig. 1 are obtained from the truncation at the second approximant (eqns (12) and (13)) with parameters as in the figure caption chosen to produce a particular combination of two loss peaks, one broader in half peak height and smaller in amplitude than the other. The first peak appears at the lower frequency, and fig. (1b) shows that its associated permittivity dispersion does not cut the abscissa, in contrast (curve I) to the higher frequency peak. In curves 2 of fig. (1) the spectrum is broadened and flattened by adjustment of one of the $\gamma$ parameters (see caption). The equivalent power reflectivity curves for a thin film of $10^{-4}$ cm on Al substrate are illustrated for the equivalent curves 1 and 2 of figs. (1a) and (1b) in fig. (1c). This is shown at the Brewster angle in pi polarisation. The equivalent results in sigma polarisation are unity for all frequencies. The high frequency feature which is the subject of this paper is visible in fig. (1c) for the higher frequency (46 $cm^{-1}$) peak of fig. (1a) at the frequency (183 $cm^{-1}$) at which the dielectric dispersion of fig. (1b) cuts the abscissa from the negative to the positive. The equivalent feature in pi polarisation is the inverted peak at 183 $cm^{-1}$ clearly visible in fig. (1c). Note that the position of the original

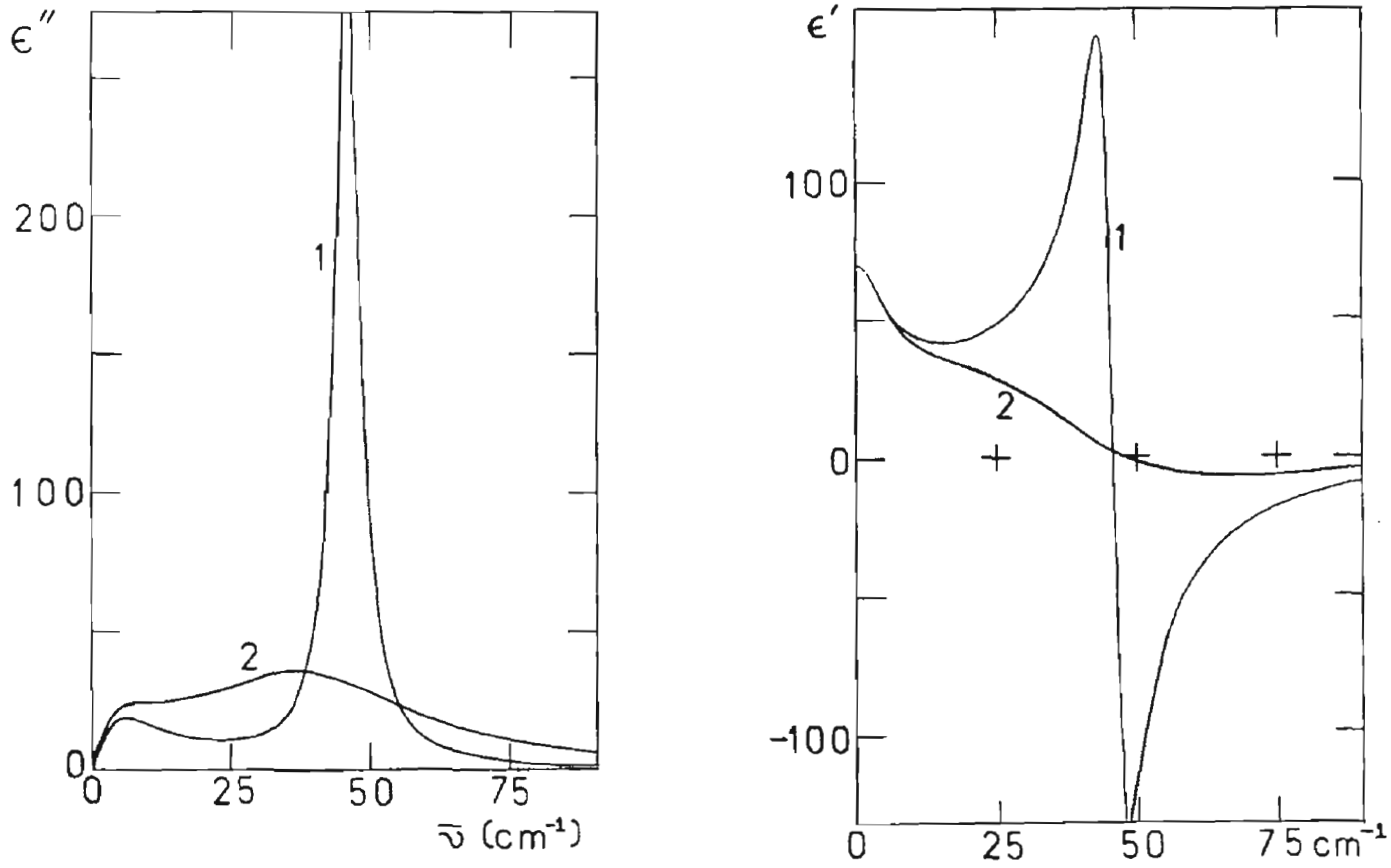


Fig. 1.

a) Two peak spectrum for the dielectric loss from Mori two variable theory.

1 $\gamma_1^{(1)} = 10^{13}s^{-1}$; $\phi_o^{(1)} = 10^{25}s^{-2}$; $\gamma_1^{(2)} = 10^{12}s^{-1}$; $\phi_o^{(2)} = 7.5 \times 10^{25}s^{-2}$

2 $\gamma_1^{(1)} = 10^{13}s^{-1}$; $\phi_o^{(1)} = 10^{25}s^{-2}$; $\gamma_1^{(2)} = 10^{13}s^{-1}$; $\phi_o^{(2)} = 7.5 \times 10^{25}s^{-2}$.

b) As for a) the dielectric permitivity.

loss maximum for this higher frequency peak is marked in pi reflectivity only by a small residual blip at 46 $cm^{-1}$ (fig. (1c)). Furthermore the secondary high frequency peak in pi reflectivity is not observed for the lower frequency loss peak at 6 $cm^{-1}$ in fig. (1a). This proves that the "blue shift" in pi reflectivity is there only when the permittivity cuts the axis from negative to positive. In general this only occurs for infra-red peaks that are sharp enough to promote the characteristic positive to negative property illustrated for the higher frequency peak of curve 1 of fig. (1a). Under the conditions of fig. (1c) it is interesting to note however that there is a red shift in pi reflectivity for the lower frequency peak of fig. (1a). This red-shift is the inverted peak around zero frequency in fig. (1c), which is in fact almost full scale and dominates the pi reflectivity in the microwave. As noted in great detail elsewhere [2] many different patterns of reflectivity

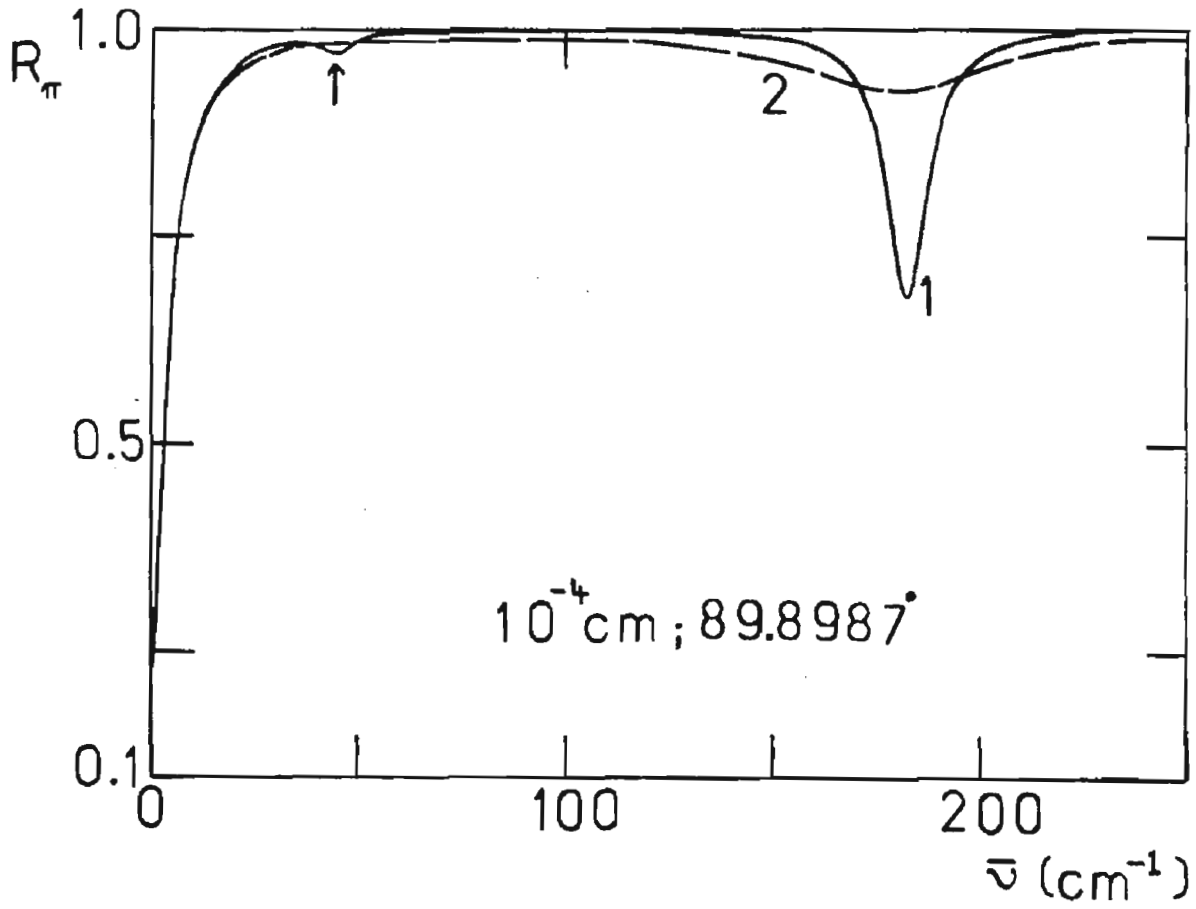


Fig. 2. Power reflectivity coefficients in sigma and pi polarisation from the dielectric loss and permittivity of fig. (1) for a layer of surface material $10^{-4}$ cm thick at an angle of incidence of 89.8987°.

are obtained under different conditions of surface film thickness, incidence angle, and substrate optical properties, thus giving considerable scope for the development of a new and precise analytical method.

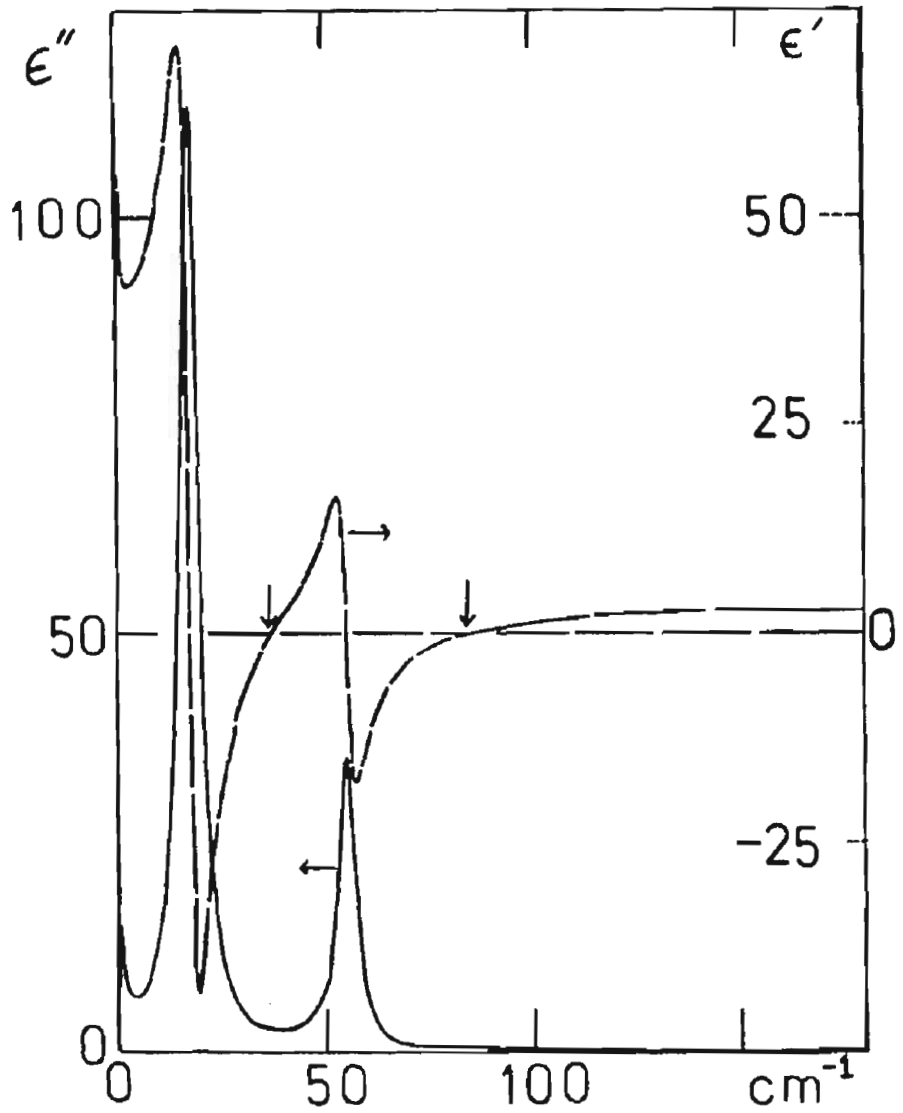


Fig. 3. Dielectric loss (full curves) and permittivity (dashed curve) for the peak spectrum generated from the Mori three variable theory with parameters

$$\gamma_2^{(1)} = 10^{13}s^{-1};\quad \phi_o^{(1)} = 10^{25}s^{-2};\quad \phi_1^{(1)} = 10^{25}s^{-2}$$

$$\gamma_2^{(2)} = 10^{12}s^{-1};\quad \phi_o^{(2)} = 10^{25}s^{-2};\quad \phi_1^{(2)} = 10^{26}s^{-2}$$

(see text). The l.h. ordinate defines the dielectric loss and the r.h. ordinate scale the permittivity. The two vertical arrows mark the points at which the permittivity cuts the axis from negative to positive.

The effect of broadening the two peaks in fig. (1), thus generating curves (2) of that figure, is to "wash out" the blue shift in fig. (1c) while retaining the red shift almost unchanged. We therefore call this new feature the Leveller effect.

In fig. (3) the Mori three variable series, eqns (14) and (15), is used to generate a clearly peaked dielectric loss spectrum whose permittivity dispersion crosses the negative to positive axis twice (as indicated by the arrows in the figure). This spectrum is generated by the parameters in the figure caption. The spectrum of fig. (3) is a typical infra-red spectrum comprised of sharp peaks when the dielectric loss is converted to power absorption. The spectrum in fig. (3) is synthesised to illustrate the effect of the change of sign from negative to positive in the dielectric permittivity on the power reflectivity. For practical applications this could be important in the detection and analysis of low dimensional layers on metal and other substrates. For example, in fig.

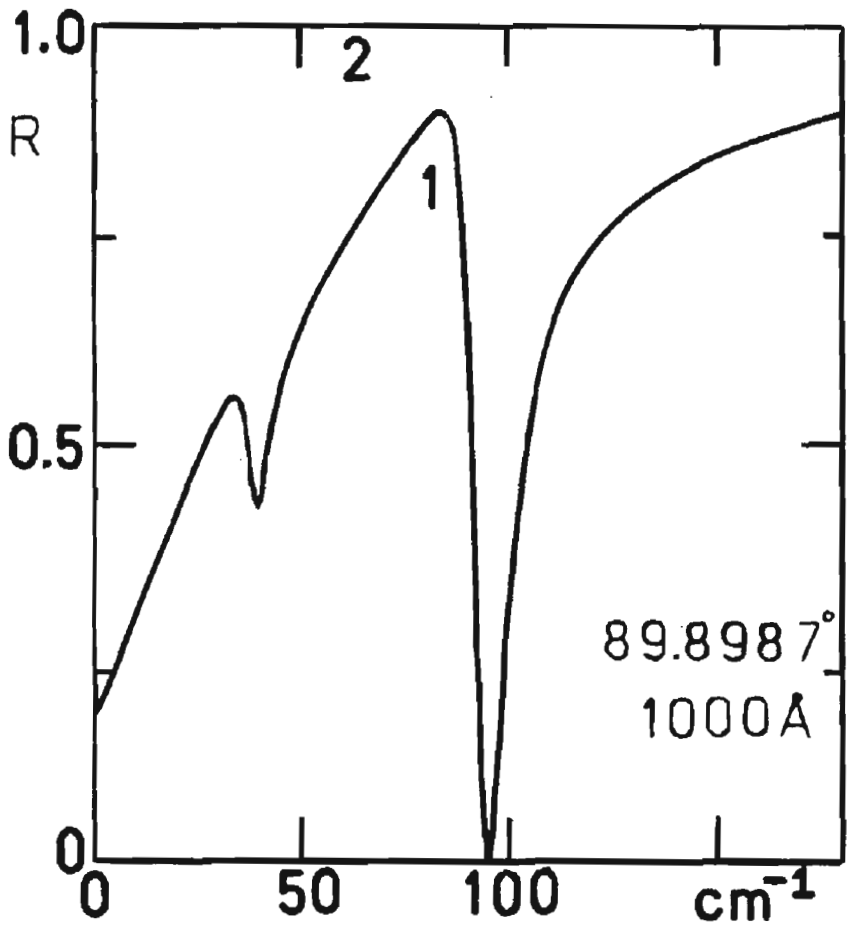


Fig. 4. Power reflectivity in pi polarisation (I) and in sigma (2) from the complex frequency dependent polarisability of fig. (3).

(4) the power reflectivity in pi polarisation for a 1000 Å layer is illustrated at the Brewster angle, 89.8987°. The material in the layer has the dielectric loss and permittivity of fig. (3). In fig. (4) the frequencies marked by arrows in fig. (3) have been transformed into two distinct dips, the higher frequency one being amplified amost to full scale. In contrast the power reflectivity in sigma polarisation (curve 2 of fig. (4)) is unity for all frequencies and cannot be used to analyse the spectral properties of the thin surface layer. Curve (1), in pi polarisation, clearly shows however that in pi polarisation the analysis of the layer would be a fairly straightforward matter, provided that the beam of the interferometer is accurately collimated and the angle of incidence is sufficiently close to the Brewster angle. The interesting high frequency features in fig. (3) are therefore maintained in the pi reflectivity spectrum of fig. (4) when there is more than one peak in the dielectric loss.

The type of spectrum illustrated in fig. (4) is also acutely sensitive to angle of incidence. By decreasing the angle to 85.0° (fig. (5)) the almost full

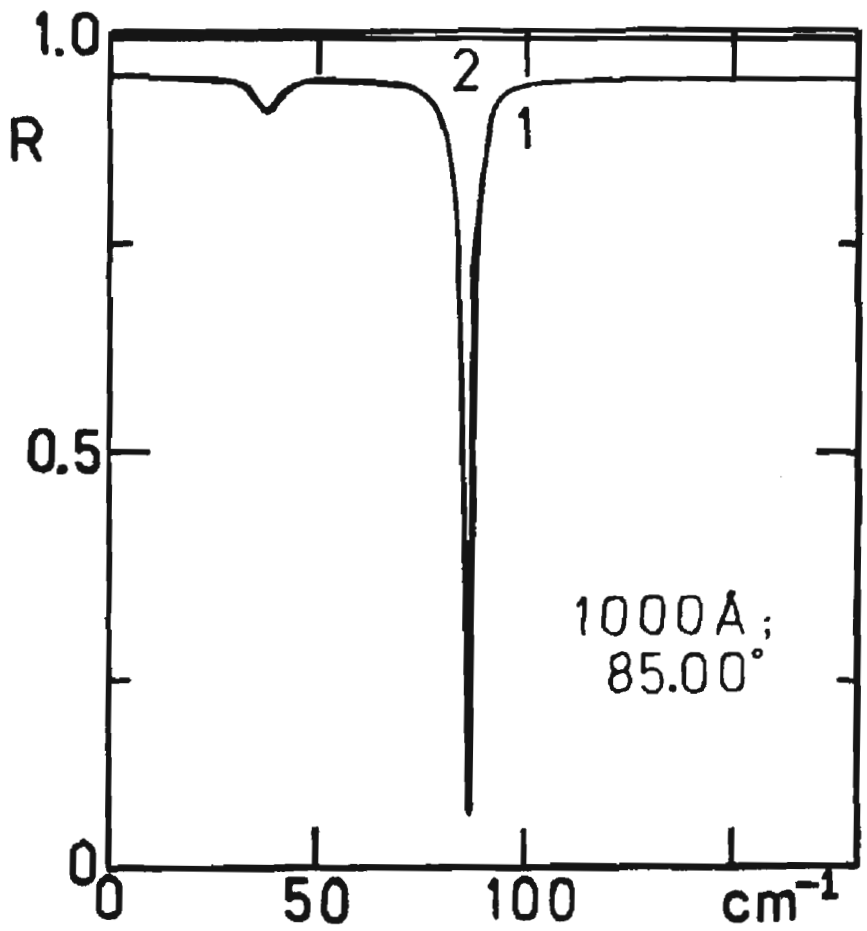


Fig. 5. Power reflectivity as for fig. (4) for the same thickness of surface layer (100 Å) and an angle of incidence of 85.00°.

scale dip around zero frequency disappears while the two inverted peaks maintain their relative intensity and frequency. An analysis of this kind of movement as a function of incidence angle gives plenty of scope for determining whether the spectral properties of the surface layer and those of the bulk material making up the layer are actually compatible. If the dielectric loss and permittivity are known as a function of frequency, the reflectivity profiles can be generated therefore as in this paper. If the theoretically expected profiles (such as those in figs (4) and (5)) do not match the actually experimentally measured profiles under the same conditions then the molecular dynamics and quantum properties of the surface layer will be different from those in the bulk. New fundamental phenomena akin to the fractional quantum Hall effect could be discovered in the infra-red reflectivity

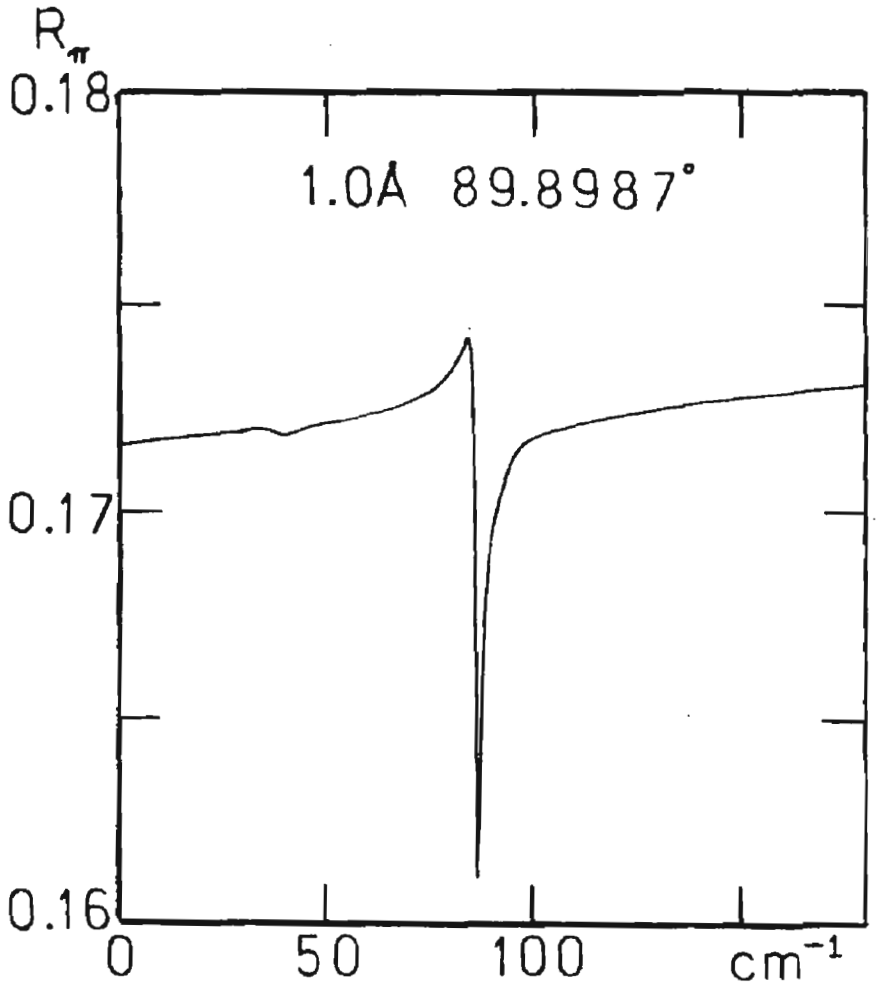


Fig. 6. Power reflectivity in pi polarisation for a layer of 1.0 Å at an incidence angle of $89.8987^{o}$ from the complex dielectric permittivity of fig. (3).

spectra of monolayers of semiconducting or epitaxial material at low (liquid helium) temperatures. Under these conditions the dielectric loss is known to be composed of sharp peaks and reflectivity features such as those in figs. (4) and (5) would appear, theoretically, for very thin layers.

Fig. (6) shows that the two features of figs. (4) and (5) are still available for analysis at the Brewster angle in pi polarisation in a surface monolayer of only 1.0 Å thickness. The higher frequency dip in fig. (6) is obviously present and the lower frequency dip is just visible on the background pi reflectivity of 0.173. This makes possible, theoretically, the detection of monolayers by infra red reflectivity in pi polarisation near the Brewster angle. Note that the reflectivity curves of figs. (4) to (6) are all generated from the same dielectric loss and permittivity (fig. (3)).

Fig. (7), for 1000 Å at 60.0°, illustrates the amplifying effect of using

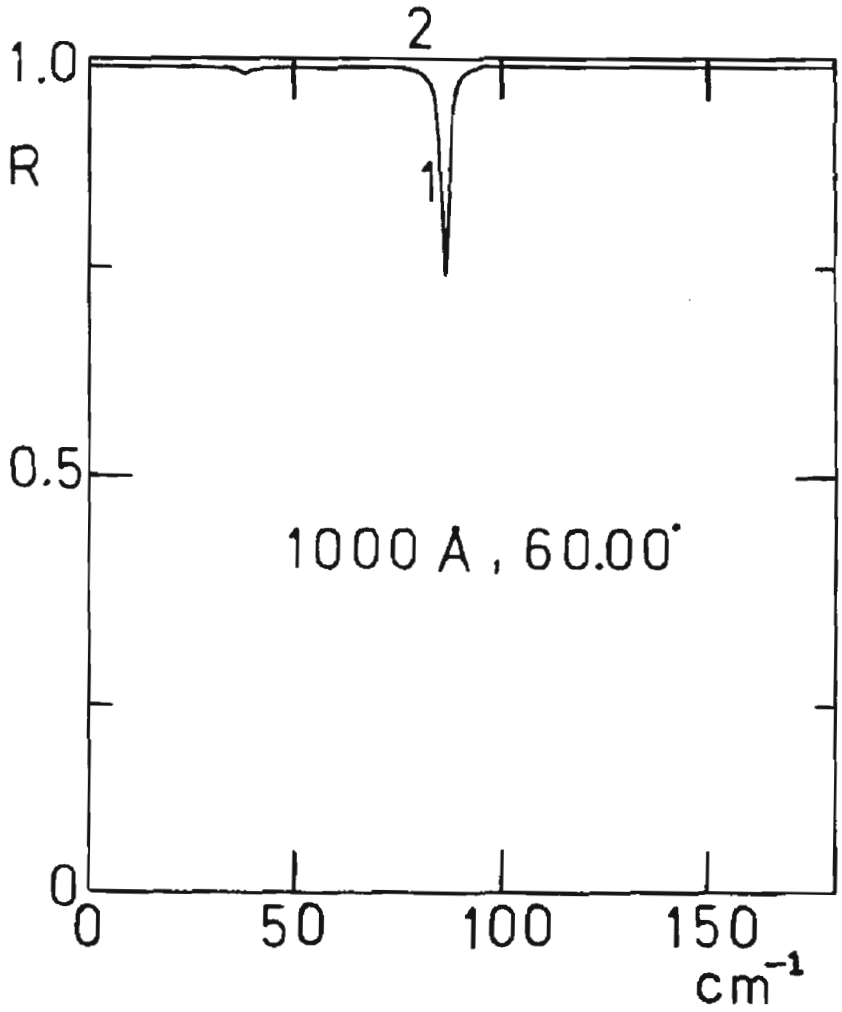


Fig. 7. Power reflectivity in pi polarisation from a 1000 Å layer on Al substrate for an incidence angle of 60.0000°.

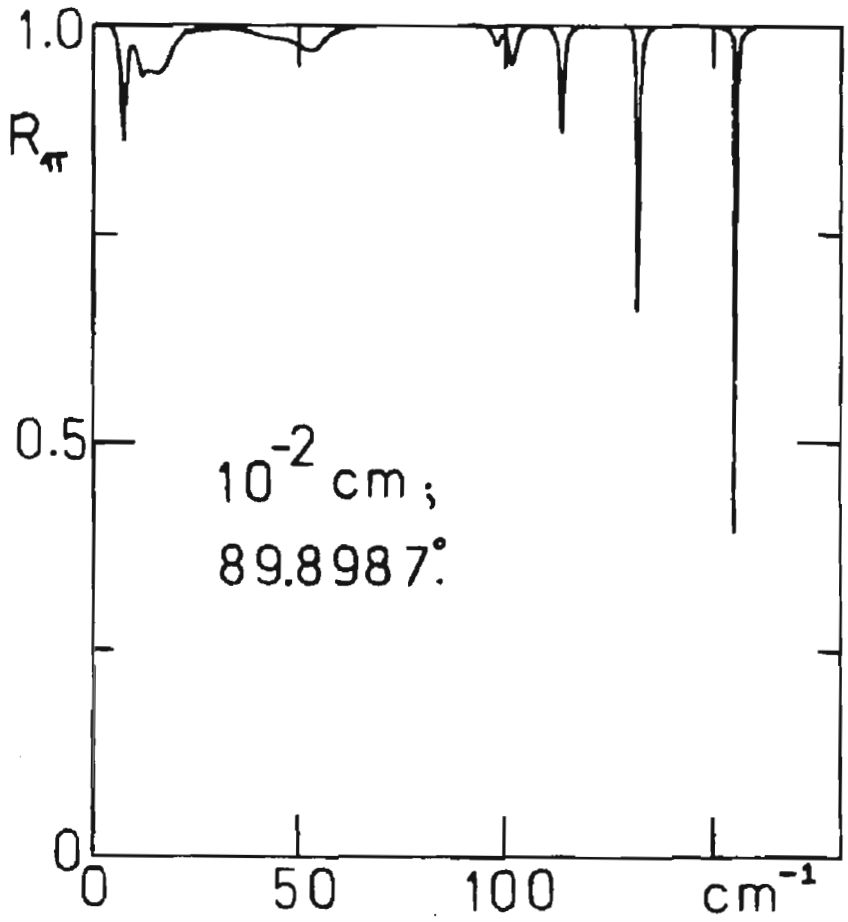


Fig. 8. Power reflectivity in pi polarisation from a thin layer of 0.01 cm on an aluminium substrate.

low angles (i.e. those near the parallel) for work of this kind. At 60.0° incidence the features in pi polarisation are much weaker for a 1000 Å layer and therefore less suitable for analysis and detection of monolayer properties. However all the information possible from the reflectivity experiment should be utilised to investigate the thoroughly spectra at a range of angles and frequencies. This is especially important when the initial absorption spectrum of the bulk material (e.g. fig. (3)) is likely to consist of many peaks.

Fig. (8), finally, shows that the dependence of the reflectivity spectrum on the thickness of the surface layer is intricate [2], and changes markedly in appearance as the thickness is increased. For single peaked dielectric loss spectra, this is discussed in full detail elsewhere [2].

ACKNOWLEDGEMENTS

The University of Wales is acknowledged for the award of the Pilcher Senior Fellowship.

REFERENCES

1 M W Evans, Chem. Phys. Letters, in press.

2 E Hild, M W Evans and G J Evans, J. Mol. Liq., submitted.

3 M.W.Evans and G J Evans, J. Mol. Liq., submitted.

4 E.Hild and M W Evans, J. Applied Phys., 59 (1986) 1147.

5 E.Hild and A. Crofscik, Infra Red Phys., 18 (1978) 23

6 E. Hild, Doctoral Dissertation, Univ. of Budapest, Hungary.

7 M.W. Evans, G.J. Evans, W.T. Coffey and P. Grigolini, "Molecular Dynamics" (Wiley/Interscience, New York, 1982), p. 258.

8 E. Shiles, T. Sasaki, M. Inokuti and D.Y. Smith, Phys. Rev. B, 22 (1980)1612

9 "Memory Function Approaches to Stochastic Problems in Condensed Matter", vol 62 of "Advances in Chemical Physics" ed. M.W. Evans, P. Grigolini, and G. Pastori Parravicin ser. ed. I. Prigogine and S.A. Rice, (Wiley/ Interscience, New York, 1985).